Chemical Science

EDGE ARTICLE

View Article Online
View Journal | View Issue

Cite this: *Chem. Sci.*, 2016, **7**, 1142

Negative ion photoelectron spectroscopy confirms the prediction that D_{3h} carbon trioxide (CO_3) has a singlet ground state†

David A. Hrovat,[a] Gao-Lei Hou,[b] Bo Chen,[a] Xue-Bin Wang*[b] and Weston Thatcher Borden*[a]

Received 19th September 2015
Accepted 2nd November 2015

DOI: 10.1039/c5sc03542b

www.rsc.org/chemicalscience

The CO_3 radical anion ($CO_3^{\bullet-}$) has been formed by electrospraying carbonate dianion (CO_3^{2-}) into the gas phase. The negative ion photoelectron (NIPE) spectrum of $CO_3^{\bullet-}$ shows that, unlike the isoelectronic trimethylenemethane [$C(CH_2)_3$], D_{3h} carbon trioxide (CO_3) has a singlet ground state. From the NIPE spectrum, the electron affinity of D_{3h} singlet CO_3 was, for the first time, directly determined to be EA = 4.06 ± 0.03 eV, and the energy difference between the D_{3h} singlet and the lowest triplet was measured as $\Delta E_{ST} = -17.8 \pm 0.9$ kcal mol^{-1}. B3LYP, CCSD(T), and CASPT2 calculations all find that the two lowest triplet states of CO_3 are very close in energy, a prediction that is confirmed by the relative intensities of the bands in the NIPE spectrum of $CO_3^{\bullet-}$. The 560 cm^{-1} vibrational progression, seen in the low energy region of the triplet band, enables the identification of the lowest, Jahn–Teller-distorted, triplet state as $^3A_1$, in which both unpaired electrons reside in σ MOs, rather than $^3A_2$, in which one unpaired electron occupies the b_2 σ MO, and the other occupies the b_1 π MO.

Introduction

Carbon trioxide, CO_3, is an unusual molecule with a long history. In 1962 CO_3 was proposed by Katakis and Taube to be an intermediate in photoreaction of O_3 with CO_2.[1] Four years later, CO_3 was again postulated as a reactive intermediate, this time in the photoreaction of CO_2 with itself.[2]

Experimental confirmation of the existence of CO_3 was obtained by IR spectroscopy on the matrix-isolated molecule, first by Moll, Clutter and Thompson in 1966,[3] and subsequently by Weissberger, Breckenridge and Taube in 1967 (ref. 4) and by Jacox and Milligan in 1971.[5] These experiments favored a C_{2v} structure for CO_3, containing a three-membered O–C–O ring and a carbonyl group. Nevertheless, a higher energy, D_{3h} isomer was detected by Kaiser and coworkers in 2006.[6] Very recently, the C_{2v} and D_{3h} isomers were reported by Sivaraman and coworkers to coexist in ion-irradiated CO_2 ice.[7]

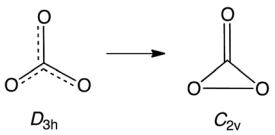

A number of theoretical studies from the 1960s to 1980s investigated the structure of CO_3, mainly focusing on relative stabilities of the cyclic C_{2v} structure, the acyclic C_s structure, and the linear $C_{\infty v}$ structure.[8] These INDO, EH, SCF, and MP2 calculations all found that the C_{2v} isomer is the lowest in energy.[9]

Nevertheless, in 1987 CISD calculations by Mulder and coworkers found the D_{3h} structure to be lower in energy than the C_{2v} structure.[10] However, subsequent calculations at higher levels of theory agree that the ground state of CO_3 possesses a C_{2v} structure, which is computed to be 1.8–6.4 kcal mol^{-1} lower in energy than the D_{3h} isomer.[11] A small barrier of 4.0–8.6 kcal mol^{-1} is calculated for the isomerization from the C_{2v} to D_{3h} structure.[11b,e,12] The computational finding of separate C_{2v} and D_{3h} minima, with the former lower in energy than the latter, is, of course, consistent with the results of the experiments on matrix-isolated CO_3.[3–7]

The singlet-triplet energy difference (ΔE_{ST}) in CO_3 has also been computed. ΔE_{ST} between the $^1A_1$ singlet ground state and the $^3A_1$ triplet state at their C_{2v} equilibrium geometries was

[a]*Department of Chemistry and the Center for Advanced Scientific Computing and Modeling, University of North Texas, 1155 Union Circle, #305070, Denton, Texas 76203-5017, USA. E-mail: borden@unt.edu*

[b]*Physical Sciences Division, Pacific Northwest National Laboratory, P. O. Box 999, MS K8-88, Richland, WA 99352, USA. E-mail: xuebin.wang@pnnl.gov*

† Electronic supplementary information (ESI) available: Optimized geometries, electronic energies, zero-point vibrational energies, and imaginary frequencies for all of the CO_3 electronic states discussed in this manuscript, computed with the aug-cc-pVTZ basis set, using B3LYP, CCSD(T), and (16/13)CASPT2 calculations. Fig. S1 contains the CCSD(T) simulation of the triplet region of the NIPE spectrum of $(CO)_3^{\bullet-}$ and the assignment of the vibrational progressions in it; Fig. S2 shows the calculated NIPE spectrum, with the lines in the stick spectrum in Fig. S1, convoluted with Gaussians; and Fig. S3 shows how the appearance of the simulation in Fig. 3 is modified by choosing a different value of the energy difference between the 0–0 bands in the two lowest energy triplet states (9 pages). See DOI: 10.1039/c5sc03542b

calculated by fourth-order MBPT calculations to be −20.5 kcal mol^{-1}.[11a] (The negative sign indicates that the singlet is lower in energy than the triplet). Similar values were obtained by QCISD(T) calculations.[11b,g] The ΔE_{ST} of CO_3 between the $^1A_1$ singlet state and a different triplet state ($^3B_2$) was computed to be −22.5 kcal mol^{-1} at the MRCI+Q(16,13)/6-311+G(3df)//CASSCF(16,13)/6-311G(d) level of theory.[12]

Also of interest have been the roles of CO_3 in the quenching of the singlet excited state of oxygen atom (^1D) by CO_2 and in the ^{18}O enrichment in CO_2 in the atmospheres of Earth and Mars.[13] Singlet and triplet potential energy surfaces for the reaction of O with CO_2 have both been calculated.[9,11b,14]

Our own interest in CO_3 comes from the fact that it is the n = 3 member of the isoelectronic series of $C(CH_2)_{3-n}O_n$ diradicals, for which n = 0 is trimethylenemethane (**TMM**) and n = 1 is oxyallyl (**OXA**). Negative ion photoelectron spectroscopy (NIPES) has shown that the substitution of the oxygen in **OXA** for one CH_2 group in **TMM** changes ΔE_{ST} by 17.5 kcal mol^{-1}, from ΔE_{ST} = 16.2 kcal mol^{-1} for the triplet ground state of **TMM**[15] to ΔE_{ST} = −1.3 kcal mol^{-1} for the singlet ground state of **OXA**.[16]

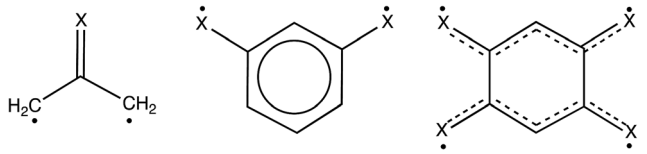

TMM, X = CH_2 **OXA**, X = O | **MBQDM**, X = CH_2 **MBQ**, X = O | **TMB**, X = CH_2 **TOTMB**, X = O

However, the substitution of oxygen for CH_2 does not always have such a large effect on ΔE_{ST} in diradicals. For example, NIPES has shown that substitution of the oxygens in *meta*-benzoquinone (**MBQ**) for both CH_2 groups in *meta*-benzoquino-dimethane (**MBQDM**) changes ΔE_{ST} by only 0.6 kcal mol^{-1}, from ΔE_{ST} = 9.6 kcal mol^{-1} in **MBQDM**[17] to ΔE_{ST} = 9.0 kcal mol^{-1} in **MBQ**.[18] Substituting the oxygens in 1,2,4,5-tetraoxatetramethylenebenzene (**TOTMB**) for the four methylene groups in tetramethylenebenzene (**TMB**) has been predicted actually to destabilize the singlet, relative to the triplet, decreasing ΔE_{ST} by 2.7 kcal mol, from a calculated value of ΔE_{ST} = −6.2 kcal mol^{-1} in **TMB** to a value of ΔE_{ST} = −3.5 kcal mol^{-1}, both calculated for and subsequently found by NIPES in **TOTMB**.[19]

As mentioned above, calculations have predicted a singlet ground state with C_{2v} geometry for CO_3, with ΔE_{ST} values ranging from −18.3 kcal mol^{-1} (ref. 11*b*) to −22.5 kcal mol^{-1}.[12] However, an experimental measurement of ΔE_{ST} in CO_3 has not been published.

Similarly, the electron affinity (EA) of CO_3 has been computed, with the best values ranging from EA = 3.84 eV to EA = 4.08 eV.[20] However, the EA of CO_3 has not been directly measured. With one exception,[21] the experimental estimates are in the range EA = 1.8–3.5 eV,[22] far below the best calculated values.[20]

In order to obtain accurate experimental values for both EA and ΔE_{ST} in CO_3, we sought to obtain the NIPE spectrum of $CO_3^{\bullet-}$. Herein we report this spectrum and assign the peaks in it with the help of DFT and *ab initio* calculations. The NIPE spectrum and our analysis of it lead to values of EA = 4.06 ± 0.03 eV, and ΔE_{ST} = −0.77 ± 0.04 eV = −17.8 ± 0.9 kcal mol^{-1} between the D_{3h} $^1A_1'$ state and the Jahn–Teller distorted $^3E'$ state.

Experimental methodology

The NIPES experiments were performed with an apparatus that consisted of an electrospray ionization source, a cryogenic ion trap, and a magnetic-bottle time-of-flight (TOF) photoelectron spectrometer.[23] Electrospraying an aqueous methanolic solution of Na_2CO_3 into a vacuum afforded generation of a weak $CO_3^{\bullet-}$ radical anion beam, although HCO_3^- was always the dominant anion formed.[24] The anions generated were guided by quadrupole ion guides into an ion trap, where they were accumulated and cooled by collisions with cold buffer gas, before being transferred into the extraction zone of a TOF mass spectrometer.

The $CO_3^{\bullet-}$ radical anions were carefully mass selected, and decelerated before being photodetached with a laser beam of 193 nm (6.424 eV) from an ArF laser in the photodetachment zone. The laser was operated at a 20 Hz repetition rate with the ion beam off at alternating laser shots, to enable shot-to-shot background subtraction to be carried out. Photoelectrons were collected at ~100% efficiency with the magnetic bottle and analyzed in a 5.2 m long electron flight tube.

The TOF photoelectron spectra were converted into electron kinetic energy spectra by calibration with the known NIPE spectra of I^- and $Cu(CN)_2^-$. The electron binding energies, given in the spectrum in Fig. 1 were obtained by subtracting the electron kinetic energies from the detachment photon energy.

The best instrumental resolution was 20 meV full width at half maximum for 1 eV kinetic energy electrons, as demonstrated in the I^- spectrum after a maximum deceleration. However, due to the weak mass intensity and light mass of $CO_3^{\bullet-}$, the NIPE spectra of $CO_3^{\bullet-}$ were obtained under compromised conditions with 4% energy resolution, *i.e.*, 40 meV for 1 eV kinetic energy electrons.

Computational methodology

In order to help analyze the NIPE spectrum of $CO_3^{\bullet-}$, three different types of electronic structure calculations were

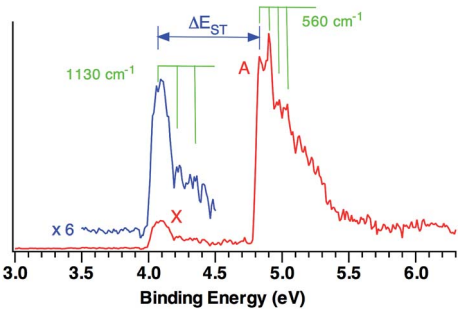

Fig. 1 The 20 K NIPE spectrum of $CO_3^{\bullet-}$ at 193 nm (6.424 eV). The intensity of the low binding energy band X is *ca.* one sixth of the high binding energy band A. The inset in blue is the X band enlarged by a factor of 6. The spectrum yields values of EA = 4.06 ± 0.03 eV, and ΔE_{ST} = −0.77 ± 0.04 eV = −17.8 ± 0.9 kcal mol^{-1}.

performed – B3LYP DFT calculations,[25] CCSD(T) coupled cluster calculations,[26] and (16/13)CASPT2 calculations.[27] In the CASPT2 calculations second-order perturbation theory was used to add the effects of dynamic electron correlation[28] to a (16/13)CASSCF wavefunction. The (16/13)CASSCF active space consisted of all the configurations that can be generated by distributing four valence electrons from carbon and four from each of the three oxygens among 13 MOs. The MOs were those formed from the σ and π 2p lone-pair AOs on each oxygen in CO_3, the three C–O bonding and three C–O antibonding σ orbitals, and the 2p–π AO on carbon.

All of the calculations were performed using the aug-cc-pVTZ basis set.[29] The B3LYP and CCSD(T) calculations and vibrational analyses at these two levels of theory were carried out using the Gaussian09 suite of programs.[30] The CASSCF and CASPT2 calculations were performed with MOLCAS.[31] The program ezSpectrum[32] was used to compute the Franck–Condon factors[33] that were necessary in order to simulate the vibrational progressions in the NIPE spectrum of $CO_3^{\bullet -}$.

Results and discussion

The NIPE spectrum of $CO_3^{\bullet -}$

Fig. 1 shows the 20 K NIPE spectrum of $CO_3^{\bullet -}$ at 193 nm. A weak band, X, peaked at electron binding energy (EBE) of ~4.1 eV, and a strong band A, peaked at EBE of ~4.9 eV, are observed in the spectrum. The intensity of the X band is *ca.* one sixth of the A band.

For statistical reasons, formation of a triplet state is a factor of three more probable than formation of a singlet state; so triplet states invariably give the most intense peaks in NIPE spectra.[34] Thus, the NIPE spectrum of $CO_3^{\bullet -}$ indicates that the ground state of CO_3 is a singlet and that the lowest excited state is a triplet. However, the factor of about six difference between the intensities of the X and A bands in the NIPE spectrum in Fig. 1 suggests that CO_3 has two triplet states with very similar energies and that both can be formed in the photodetachment of an electron from $CO_3^{\bullet -}$.

From the rising edge of the X band, we estimate the adiabatic detachment energy (ADE) of $CO_3^{\bullet -}$ (or, equivalently, the electron affinity, EA of CO_3) to be 4.06 ± 0.03 eV. The EA of CO_3 has been the subject of many previous experimental studies;[22] but our NIPES value is considerably larger than all but one of these experimental estimates.[21] However, our value of EA = 4.06 ± 0.03 eV is within experimental error of the value of EA = 4.08 eV, calculated at the CCSD(T)/aug-cc-pVTZ level by Cappa and Elrod in 2001.[20]

The experimental singlet–triplet gap of CO_3, ΔE_{ST}, is defined as the difference between the EBE of the X band (EBE = 4.06 ± 0.03 eV) and the EBE of the first resolved peak in the A band (EBE = 4.83 ± 0.03 eV). Therefore, $\Delta E_{ST} = -0.77 \pm 0.04$ eV = -17.8 ± 0.9 kcal mol^{-1} is obtained from the NIPE spectrum in Fig. 1.

Vibrational structure can be discerned in both the X and A bands. The ground state X band shows a vibrational progression with a frequency of 1130 cm^{-1}. This frequency is high enough that it is likely to belong to a C–O stretching, rather than to an O–C–O bending mode.

The vibrational mode that appears to be excited in the A band transition has a frequency of 560 cm^{-1}. Its low frequency makes it much more likely to be due to an O–C–O bending mode than to a C–O stretching mode.

The electronic structure of CO_3 – qualitative considerations

Understanding the NIPE spectrum of $CO_3^{\bullet -}$ requires understanding the electronic structure of CO_3. As already noted, D_{3h} **TMM** and D_{3h} CO_3 are isoelectronic. Therefore, like D_{3h} **TMM**, D_{3h} CO_3 might have been expected to have a triplet ground state. However, as discussed in the previous section, the NIPE spectrum of $CO_3^{\bullet -}$ shows that the ground state of D_{3h} CO_3 is a singlet and that $\Delta E_{ST} = -17.8 \pm 0.9$ kcal mol^{-1}.

The reason that **TMM** has a triplet ground state is that in D_{3h} **TMM** two electrons occupy two degenerate, e″, π MOs. The MOs are non-disjoint;[35] therefore, as expected from Hund's rule,[36] the triplet is the electronic state of lowest energy.[16]

However, the C–H bonds in D_{3h} **TMM** are replaced by σ lone pairs of electrons on the three oxygens of CO_3. As shown in Fig. 2, the a_2' combination of oxygen lone pair orbitals is antibonding between all three oxygens. Therefore, in the lowest electronic state of D_{3h} CO_3, the a_2' MO is left empty.

The pair of electrons that occupy the a_2' C–H bonding MO in D_{3h} **TMM** reside in one of the pair of e″ π MOs in D_{3h} CO_3. Consequently, a total of four electrons occupy the e″, π MOs in D_{3h} CO_3, and four more electrons occupy the degenerate pair of e′, σ MOs. This is the reason why the lowest electronic state of D_{3h} CO_3 is a closed-shell singlet.

In the $CO_3^{\bullet -}$ radical anion one electron occupies the a_2' MO. In the low energy triplet states of neutral CO_3 one electron in the closed-shell, singlet, ground state is excited into this MO.

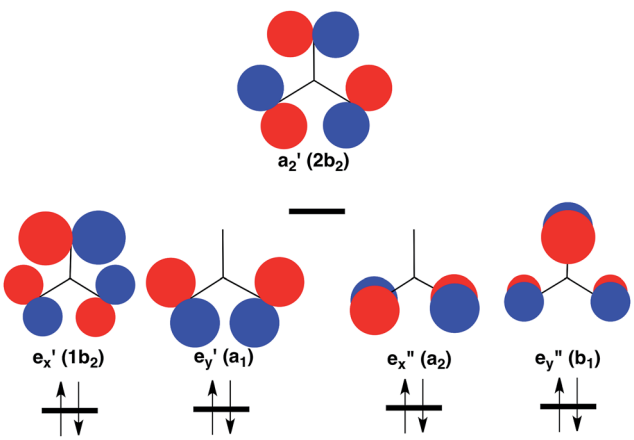

Fig. 2 Schematic depiction of the three σ and two π lone-pair MOs of highest energy that are localized on the three oxygens in CO_3. Symmetries of these MOs are given at D_{3h} and (C_{2v}) geometries. Of these MOs, a_2' is highest in energy, because it contains antibonding σ interactions between all three oxygens. Therefore, a_2' is left empty and the degenerate pairs of e′ and e″ MOs are each doubly occupied in the closed-shell singlet ground state of CO_3.[37] The orbital occupancy in this $^1A_1'$ state is indicated at the bottom of Fig. 2.

Table 1 Calculated B3LYP,[25] CCSD(T),[26] and CASPT2 (ref. 27) energies (kcal mol^{-1}) of the ground state of $CO_3^{\bullet -}$ and of the low-lying electronic states of CO_3, relative to the D_{3h} $^1A_1'$ state of CO_3. Calculations were carried out with the aug-cc-pVTZ basis set.[29] Electronic states and orbital occupancies after Jahn–Teller distortions to C_{2v} symmetry of the two components of $^3E'$ and $^3E''$ states are given in parentheses, and the energies after the Jahn–Teller distortions are indicated by arrows

Electronic state	B3LYP	CCSD(T)	CASPT2
$^2A_2'$ of $CO_3^{\bullet -}$	−116.4 (−5.05 eV)	−95.4 (−4.13 eV)[a]	−93.9 (−4.07 eV)
$^1A_1'$ (D_{3h} minimum)	0	0[b]	0
$^1A_1$ (C_{2v} TS)[c]	0.6	1.5	6.6
$^1A_1$ (C_{2v} minimum containing an O–C–O ring)	−13.4	−5.5	−2.2
$^3E_x'$ ($^3B_2 = \|\ldots a_1^{\alpha}2b_2^{\alpha}\rangle$)	−1.0 → −4.2	19.1 → 16.3	24.8 → 21.0
$^3E_y'$ ($^3A_1 = \|\ldots 1b_2^{\alpha}2b_2^{\alpha}\rangle$)	−1.0 → −3.6	18.6 → 15.5	23.7 → 20.8
$^3E_x''$ ($^3A_2 = \|\ldots b_1^{\alpha}2b_2^{\alpha}\rangle$)	1.0 → −1.0	19.5 → 17.8	20.1 → 19.8
$^3E_y''$ ($^3B_1 = \|\ldots a_2^{\alpha}2b_2^{\alpha}\rangle$)	−0.6 → −0.7	19.5 → 19.2	20.2 → 19.3
$^3A_2'$ ($^3B_2 = \|\ldots b_1^{\alpha}a_2^{\alpha}\rangle$)	11.7	28.4	35.9

[a] Previous calculations at this level of theory obtained −4.08 eV for the EA of CO_3.[20] [b] Artifactual symmetry breaking[39–41] results in this state having two imaginary frequencies for distortions that lead to three equivalent C_{2v} minima. These minima have CCSD(T) energies that are 0.9 kcal mol^{-1} lower than that of the D_{3h} singlet state. [c] One of three transition structures that connect the D_{3h} singlet to one of the three C_{2v} structures that are the global minima on the potential energy surface for the lowest singlet state of CO_3.

However, whether the electron that occupies the a_2' MO in the triplet comes from one of the e′ σ MOs or one of the e″ π MOs in the singlet is not obvious. The question of the relative energies of the resulting $^3E'$ and $^3E''$ states of CO_3 has been addressed by the calculations that are described in a later section of this paper.

Computational results for the lowest singlet state of CO_3

The results of our B3LYP, CCSD(T), and CASPT2 calculations on $CO_3^{\bullet -}$ and CO_3 are summarized in Table 1. All of these calculations find that in the lowest electronic state of the radical anion the unpaired electron occupies the a_2' MO, so that $CO_3^{\bullet -}$ maintains D_{3h} symmetry.[38] The B3LYP and CASPT2 calculations find that the D_{3h} singlet state is also an energy minimum.

However, the CCSD(T) calculations find that the D_{3h} geometry of the $^1A_1'$ state has two imaginary frequencies of 472i cm^{-1}. These correspond to a degenerate pair of e′ vibrations that lead to a trio of slightly distorted structures with C_{2v} symmetry (not to be confused with the cyclic C_{2v} structure with an O–C–O ring and a carbonyl group). The three equivalent C_{2v} structures are 0.9 kcal mol^{-1} lower in energy than the D_{3h} structure at the CCSD(T)/aug-cc-pVTZ level of theory.

When the basis set is expanded to aug-cc-pVQZ, the energy difference between the D_{3h} and C_{2v} structures drops to only 0.3 kcal mol^{-1}. Since the B3LYP and the CASPT2 calculations both find the D_{3h} structure to be an energy minimum, we believe that the small geometry distortions to structures with C_{2v} symmetry in the CCSD(T) calculations are due to artifactual symmetry breaking in the CCSD(T) wave function for the $^1A_1'$ state at D_{3h} geometries.[39–41]

If the lowest electronic states of $CO_3^{\bullet -}$ and CO_3 both have D_{3h} symmetry, it is possible to assign the vibrational progression in the X band of the NIPE spectrum in Fig. 1 to a symmetrical C–O stretching mode. Only vibrational modes that preserve those symmetry elements that the electronic states of the radical ion and the neutral molecule have in common are seen in NIPE spectra. Therefore, the vibrational progression with a frequency of 1130 cm^{-1} that is seen in the X band in Fig. 1 must belong to the a_1' vibration of D_{3h} CO_3.

On going from the $CO_3^{\bullet -}$ radical anion to neutral CO_3 the C–O bond lengths are calculated to shorten by 0.013 Å (CASPT2), 0.015 Å [CCSD(T)], and 0.023 Å (UB3LYP). Consequently, the calculated Franck–Condon factors predict that an a_1' C–O bond stretching vibrational progression should be seen in the X band in Fig. 1. The calculated harmonic frequencies for the a_1' C–O stretching vibration are 1083 cm^{-1} (CASPT2), 1090 cm^{-1} [CCSD(T)] and 1140 cm^{-1} (B3LYP). The B3LYP value differs by only 10 cm^{-1} from the experimental value of 1130 cm^{-1}.

Since the 1130 cm^{-1}, a_1', C–O bond stretching mode is totally symmetric, it would not have been seen in the IR spectrum of D_{3h} CO_3 in matrix isolation. The observed, asymmetric (e′), C–O bond-stretching frequency was reported to be 1165 cm^{-1}.[6]

As shown in Table 1, and, in agreement with the results of previous calculations[11] and experiments,[3–7] B3LYP, CCSD(T), and CASPT2 all find that there is a C_{2v} singlet energy minimum, containing an O–C–O ring, that is lower in energy than the D_{3h} singlet. Not unexpectedly, the barrier height that is calculated for ring closure increases as the calculated exothermicity of this reaction decreases.

Because the D_{3h} → C_{2v} ring closure reaction requires mixing of the filled e′ MOs in Fig. 2 with the empty a_2' MO, ring closure is computed to involve passage over a barrier. This orbital mixing, which occurs on an e′ distortion from D_{3h} to C_{2v} symmetry, may be regarded as a second-order Jahn–Teller effect.[42]

For example, at C_{2v} geometries e_x' and a_2' both have b_2 symmetry and so can be mixed by an e_y distortion from D_{3h} symmetry. From inspection of the MOs in Fig. 2, one can deduce that this mixing reduces the contribution of the AOs on the two oxygens between which O–O bond formation occurs and thus makes the resulting b_2 MO much less antibonding than the e_x' MO. In fact, the b_2 MO that results from the mixing between

e_x' and a_2' MOs becomes the $2p_x$ lone-pair AO on the carbonyl group of the C_{2v} singlet energy minimum.

The large change in geometry that occurs on formation of the cyclic singlet CO_3 molecule results in the absence of overlap between its vibrational wave function and the vibrational wave function of the D_{3h} $CO_3^{\bullet -}$ radical anion. Consequently, the Franck–Condon factor for the laser-induced transition from D_{3h} $CO_3^{\bullet -}$ to the C_{2v} energy minimum of singlet CO_3 is calculated to be effectively zero. Therefore, the value of EA = 4.06 ± 0.03 eV in the NIPE spectrum corresponds to the energy difference between the D_{3h} equilibrium geometry of $CO_3^{\bullet -}$ and the local D_{3h} energy minimum of neutral singlet CO_3, not the global C_{2v} energy minimum, of singlet, CO_3.

There are two types of experimental evidence that support this conclusion. The first is that the measured EA is very close to the calculated CCSD(T) and CASPT2 energy differences in Table 1 between the D_{3h} equilibrium geometry of $CO_3^{\bullet -}$ and the local D_{3h} energy minimum of neutral CO_3. Second, as already discussed, the vibrational progression of 1130 cm^{-1} seen in the X band of the NIPE spectrum in Fig. 1 is in good agreement with that predicted by all three levels of theory for the D_{3h} local minimum.

Computational results for the lowest triplet state of CO_3

As shown in Table 1, there are two low-lying triplet states in CO_3. They are E′, in which the two unpaired electrons occupy the a_2' and e′ σ MOs, and E″, in which the second unpaired electron occupies the e″ π MO, instead of the e′ σ MO.

A third triplet, $^3A_2'$, which is the ground state of **TMM**, is calculated to be very high in energy in CO_3. In this state the e_x'' and e_y'' π MOs are each singly occupied, and the a'_2 MO is doubly occupied. As shown in Fig. 2, the a_2' MO is strongly O–O antibonding; and its double occupancy in $^3A_2'$ makes this triplet state much higher in energy than either $^3E'$ or $^3E''$, in both of which the a_2' MO is singly occupied.

Whether $^3E'$ or $^3E''$ is lower in energy is not clear from qualitative considerations. As shown in Fig. 2, the e′ MOs are weakly bonding σ MOs; whereas, the e″ MOs are non-bonding π MOs. On this basis, leaving e′ doubly occupied and having e″ singly occupied should be favored; so $^3E''$ should be lower in energy than $^3E'$.

On the other hand, two electrons of the same spin cannot simultaneously occupy the same AO. With one electron in the a_2' σ MO, having a second electron of the same spin in an e′ σ MO prevents these two electrons from ever appearing on the same atom; whereas, no such prohibition exists if the second unpaired electron occupies an e″ π MO. Consequently, although maximization of bonding is expected to favor the $^3E''$ state, minimization of electron repulsion should favor the $^3E'$ state. Which effect dominates cannot be predicted from qualitative considerations; so one has to rely on calculations for the prediction of which triplet state, $^3E'$ and $^3E''$, is lower in energy.

Table 1 shows that $^3E'$ and $^3E''$ are, in fact, calculated to be very close in energy. Both degenerate triplet states are expected to undergo first-order Jahn–Teller distortions to C_{2v} symmetry,[43] and the calculated energy differences between the two triplet states at their C_{2v} equilibrium geometries range between 1 and 3 kcal mol^{-1}.

Interestingly, the results, tabulated in Table 1, reveal that the CCSD(T) and CASPT2 calculations differ as to which triplet state is predicted to be lower in energy. The CCSD(T) calculations predict that the C_{2v} triplet, formed by exciting an electron from the pair of e′ σ MOs into the a_2' σ MO, is lower in energy than the triplet that is formed by exciting an electron from the pair of e″ π MOs into the a_2' MO. B3LYP makes the same prediction as CCSD(T). However, it should be noted that B3LYP erroneously predicts that both triplet states are lower in energy than the D_{3h} $^1A_1'$ state (Table 1).

CCSD(T) and B3LYP both predict that the $^3E'$ and $^3E''$ states have very similar energies at their respective D_{3h} geometries. However, as would be expected, removing an electron from one of the e′ σ MOs results in a larger Jahn–Teller distortion than removing an electron from one of the e″ π MOs. B3LYP, CCSD(T), and CASPT2 calculations all find that this is, in fact, the case. The larger energy lowering of the $^3E'$ state by a first-order Jahn–Teller distortion leads to the prediction by both CCSD(T) and B3LYP that the C_{2v} distorted $^3E'$ state is the lowest energy triplet state of CO_3 by 2–3 kcal mol^{-1}.

In contrast to CCSD(T), CASPT2 places $^3E''$ well below $^3E'$ at their respective D_{3h} geometries. Even though the first-order Jahn–Teller distortion to C_{2v} symmetry stabilizes $^3E'$ more than $^3E''$, the energetic advantage of $^3E''$ over $^3E'$ at their respective D_{3h} geometries prevails; and the C_{2v} distorted $^3E''$ ($^3A_2$) state is calculated to be lower in energy than the C_{2v} distorted $^3E'$ ($^3A_1$) state by 1–2 kcal mol^{-1}.

Which triplet state is lower in energy, $^3E'$ ($^3A_1$) or $^3E''$ ($^3A_2$)?

Which method, CCSD(T) or CASPT2, gives the correct answer to the question of what is the lowest triplet state of CO_3, $^3E' \rightarrow {}^3A_1$ or $^3E'' \rightarrow {}^3A_2$? As described in the following paragraphs, the NIPE spectrum in Fig. 1 indicates that the CCSD(T) prediction is correct; and, although $^3A_1$ and $^3A_2$ are very close in energy, $^3A_1$ is the lower energy of these two triplet states.

This conclusion follows from the vibrational progression seen in the low energy portion of the triplet peak. As already noted, this region of the NIPE spectrum shows a progression of 560 cm^{-1}. This vibrational frequency is too low to be associated with C–O stretching, but is the right size to be due to O–C–O bending. Our calculations indicate that only $^3A_1$ should show an O–C–O bending progression, so it must be the lower energy of the two closely-spaced triplet states.

The conclusion that only $^3A_1$ should show an O–C–O bending progression follows from the calculated geometries of $^3A_1$ and $^3A_2$ and is supported by our simulations of the vibrations in the peaks due to $^3A_1$ and $^3A_2$ in the NIPE spectra of $CO_3^{\bullet -}$. Table 2 gives the bond lengths and the unique bond angle of the C_{2v} minima to which CCSD(T) and CASPT2 both predict that $^3E'$ and $^3E''$ distort. It is clear that both the bond lengths and the bond angles of the $^3A_1$ minima of the distorted $^3E'$ state deviate significantly from the equality they have at D_{3h} geometries. However, the bond angles of the $^3A_2$ minima of the distorted $^3E''$

Table 2 Optimized bond lengths (Å) and bond angles (degs) at the C_{2v} geometries of the $^3A_1$ and $^3A_2$ states of CO_3, calculated with B3LYP, CCSD(T), and CASPT2, using the aug-cc-pVTZ basis set. O_1 is the unique oxygen, and O_2 and O_3 are the two equivalent oxygens at C_{2v} geometries

	B3LYP		CCSD(T)		CASPT2	
Bond length, or bond angle	$^3A_1$	$^3A_2$	$^3A_1$	$^3A_2$	$^3A_1$	$^3A_2$
$R(C–O_1)$	1.311	1.338	1.321	1.334	1.325	1.315
$R(C–O_2) = R(C–O_3)$	1.257	1.245	1.259	1.254	1.259	1.267
$O_2–C–O_3$	113.6°	122.0°	113.8°	119.2°	114.2°	119.7°
$O_1–C–O_2 = O_1–C–O_3$	123.2°	119.0°	123.1°	120.4°	122.9°	120.1°

state are calculated to remain much more nearly equal after Jahn–Teller distortions.

The difference between the geometries of the C_{2v} minima for the two triplet states is a consequence of the difference between the MOs that are occupied in these two states. In the $^3A_1$ state an electron, which occupies the $1b_2$ σ MO in the D_{3h} $^1A_1'$ ground state, is removed and placed in the $2b_2$ σ MO. As shown in Fig. 2, this electronic excitation results in the $O_1–O_2$ and $O_1–O_3$ σ bonding interactions in the $1b_2$ MO being replaced by σ antibonding interactions between all of the oxygens in the $2b_2$ MO. Consequently, the $O_1–C–O_2$ and $O_1–C–O_3$ bond angles in $^3A_1$ are calculated to be larger than 120°; so the $O_2–C–O_3$ bond angle is predicted to be much less than 120° in this state.

In the $^3A_2$ state an electron, which occupies the b_1 π MO in the D_{3h} $^1A_1'$ ground state, is removed and placed in the $2b_2$ σ MO. The antibonding $O_1–O_2$ and $O_1–O_3$ π interactions in b_1 are lost, as is the bonding $O_2–O_3$ π interaction. Consequently, the $O_1–C–O_2$ and $O_1–C–O_3$ angles in the $^3A_2$ state are expected to be less than 120°, and the $O_2–C–O_3$ angle is expected to be greater than 120°.

These qualitative expectations are fulfilled at the B3LYP level of theory. However, because the 1,3-interactions between the oxygens in $^3A_2$ involve π, rather than σ AOs, the deviations of the B3LYP bond angles from 120° are about three times smaller in $^3A_2$ than in $^3A_1$. In fact, the π interactions in $^3A_2$ are so small that, in the optimized CCSD(T) and CASPT2 geometries, the deviations of the bond angles from 120° are not only less than 1° but they actually deviate from 120° in the opposite direction from the B3LYP bond angles.

In NIPE spectra progressions are only seen in vibrational modes that affect the geometrical parameters by which an electronic state differs from the radical anion from which the electronic state is formed.[34] The calculated O–C–O bond angles in the $^3A_1$ state of CO_3 differ significantly from those in the D_{3h} equilibrium geometry of the $^2A_2'$ ground state of $CO_3^{\bullet-}$. Therefore, one would expect to see a long vibrational progression in O–C–O bending in the band for formation of the $^3A_1$ state of CO_3 in the NIPE spectrum of $CO_3^{\bullet-}$.

On the other hand, the calculated O–C–O bond angles in the $^3A_2$ state of CO_3 are very close to those in the D_{3h} equilibrium geometry of the $^2A_2'$ radical anion. Therefore, one would not expect to see a long vibrational progression in O–C–O bending in the band for formation of the $^3A_2$ state of CO_3 in the NIPE spectrum of $CO_3^{\bullet-}$. The only long vibrational progression that should appear in the band for formation of the $^3A_2$ state is one in C–O bond stretch, since the C–O bond lengths in the C_{2v} equilibrium geometry of $^3A_2$ in Table 2 differ from those in the D_{3h} equilibrium geometry of the radical anion.[44]

Fig. 1 shows that a vibrational progression of 560 cm^{-1} in O–C–O bending is found in the band for formation of the lowest triplet state of CO_3 in the NIPE spectrum of $CO_3^{\bullet-}$. As discussed above, such a progression is expected to be seen in the $^3A_1$ state of CO_3, but not in the $^3A_2$ state. Thus, it follows that the lowest triplet state of CO_3 is the $^3A_1$ state, in which one unpaired electron resides in the $1b_2$ MO and the other resides in the $2b_2$ MO.

This qualitative conclusion is supported by both B3LYP and CCSD(T) simulations of the triplet region of the NIPE spectrum

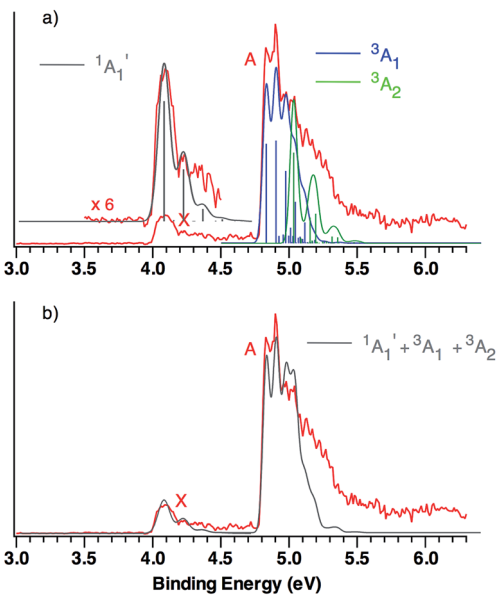

Fig. 3 (a) B3LYP/aug-cc-pVTZ calculated vibrational structure in the NIPE spectrum of $CO_3^{\bullet-}$, superimposed on the experimental NIPE spectrum (red). The positions of the bands in the calculated stick spectrum for $^1A_1'$ (grey), $^3A_1$ (blue), and $^3A_2$ (green) have been adjusted, in order to align the 0–0 bands in the calculated spectrum with the 0–0 bands in the observed spectrum. The calculated spectrum, using Gaussian line shapes with, respectively, 100, 60, and 60 meV full widths at half maxima for each stick in $^1A_1'$, $^3A_1$, and $^3A_2$, is also shown. (b) The computed NIPE spectrum (grey), calculated from the sum of the convoluted contributions of the singlet and two triplets in Fig. 3a, superimposed on the experimental 193 nm spectrum (red).

of $CO_3^{\bullet-}$. Using the Franck–Condon factors (FCFs) calculated with ezSpectrum,[32] Fig. 3 shows how the NIPE spectrum of $CO_3^{\bullet-}$ is predicted to appear, based on the results obtained with B3LYP calculations.

The predicted vibrational structure for the triplet region of the NIPE spectrum, based on the results of CCSD(T) calculations, has a very similar appearance to the B3LYP-based simulation in Fig. 3. The CCSD(T) simulations are provided in Fig. S1 and S2 of the ESI† of this manuscript, and the vibrational mode assignments are given in Fig. S1.† Both the B3LYP and CCSD(T) simulations confirm that the vibrational progressions in the triplet region of the experimental NIPE spectrum are dominated by the O–C–O bending mode in $^3A_1$ and by C–O bond stretch in $^3A_2$.

Comparison of the simulated spectra for both triplet states with the actual NIPE spectrum suggests aligning the 0–0 band of $^3A_2$ with the fourth resolved peak (EBE = 5.03 eV) in band A, which leads to the conclusion that the $^3A_2$ state is 0.20 eV (4.6 kcal mol^{-1}) higher in energy than $^3A_1$. This ordering of the two triplet states is in accordance with the results of both the B3LYP and CCSD(T) calculations (Table 1). However, an energy difference of 4.6 kcal mol^{-1} would be about twice the size of the energy differences of, respectively, 2.6 and 2.3 kcal mol^{-1} that are predicted by these two types of calculations.

An alternative alignment of the 0–0 band of $^3A_2$ with the third resolved peak (EBE = 4.97 eV) in band A is shown in Fig. S3 of the ESI.† This alignment makes the $^3A_2$ state only 0.14 eV (3.2 kcal mol^{-1}) higher in energy than $^3A_1$, which is in better agreement with the energy differences between these two states, computed by both B3LYP and CCSD(T). However, comparison of Fig. S3† with Fig. 3, shows that the alignment in Fig. S3† fits the observed intensities of the peaks in the experimental NIPE spectrum less well than the alignment in Fig. 3.

The simulated vibrational structure for formation of the singlet ground state of CO_3 is also shown in Fig. 3. The simulation reproduces well the observed vibrational progression in the singlet ground state and confirms the conclusion that this progression is due to the symmetric C–O stretching.

The simulations, based on the calculated FCFs, for formation of the singlet and two triplet states of CO_3 from the $^2A_2'$ state of $CO_3^{\bullet-}$, provide a good fit to the experimental NIPE spectrum of $CO_3^{\bullet-}$ up to 5.1 eV. There appears to be a shoulder at EBE $\sim$ 5.3 eV in the experimental spectrum, which might be due to formation of the third, low-lying triplet state, $^3A_2'$, which is predicted by the CCSD(T) calculations to have EA = 5.37 eV.

The similarity between the calculated and experimental NIPE spectra of $CO_3^{\bullet-}$ in Fig. 3 provides evidence that our assignments of the peaks in the experimental NIPE spectra are correct and that, as predicted by both B3LYP and CCSD(T), the $^3A_1$ state of CO_3 is lower in energy than the $^3A_2$ state.

Conclusions

We report the first NIPE spectrum of $CO_3^{\bullet-}$. The spectrum shows that, substitution of the three oxygens in CO_3 for the three CH_2 groups in **TMM** results in a change in the ground state, going from $^3A_2'$ and ΔE_{ST} = 16.2 kcal mol^{-1} in **TMM**[15] to $^1A_1'$ and $\Delta E_{ST} = -17.8 \pm 0.9$ kcal mol^{-1} in CO_3. The NIPE spectrum also provides the first measurement of EA = 4.06 $\pm$ 0.03 eV in D_{3h} CO_3. Qualitative MO analysis and quantitative electronic structure calculations confirm that the ground state of CO_3 is a singlet and reveal which of the two closely-spaced triplet excited states is lower in energy. The CCSD(T) and CASPT2 calculations reproduce the experimental EA and ΔE_{ST} values of CO_3 rather well.

The combined results of our experiments and calculations contribute fundamental information about the electronic structure of CO_3, a molecule that is not only of interest because it is isoelectronic with both **TMM** and **OXA**, but that is also important in both atmospheric chemistry and astrochemistry.[12–14,45]

Conflict of interest

The authors declare no competing financial interest.

Acknowledgements

The calculations at UNT were supported by Grant B0027 from the Robert A. Welch Foundation. The NIPES research at PNNL was supported by the U.S. Department of Energy (DOE), Office of Science, Office of Basic Energy Sciences, Division of Chemical Sciences, Geosciences and Biosciences and was performed at the EMSL, a national scientific user facility sponsored by DOE's Office of Biological and Environmental Research and located at Pacific Northwest National Laboratory, which is a multiprogram national laboratory operated for DOE by Battelle.

Notes and references

1 D. Katakis and H. Taube, *J. Chem. Phys.*, 1962, **36**, 416.
2 A.-Y. Ung and H. I. Schiff, *Can. J. Chem.*, 1966, **44**, 1981.
3 N. G. Moll, D. R. Clutter and W. E. Thompson, *J. Chem. Phys.*, 1966, **45**, 4469.
4 E. Weissberger, W. H. Breckenridge and H. Taube, *J. Chem. Phys.*, 1967, **47**, 1764.
5 M. E. Jacox and D. E. Milligan, *J. Chem. Phys.*, 1971, **54**, 919.
6 C. S. Jamieson, A. M. Mebel and R. I. Kaiser, *ChemPhysChem*, 2006, **7**, 2508.
7 B. Sivaraman, B. N. R. Sekhar, D. Fulvio, A. Hunniford, B. McCullough, M. E. Palumbo and N. Mason, *J. Chem. Phys.*, 2013, **139**, 074706.
8 (*a*) B. M. Gimarc and T. S. Chou, *J. Chem. Phys.*, 1968, **49**, 4043; (*b*) J. F. Olsen and L. Burnelle, *J. Am. Chem. Soc.*, 1969, **91**, 7286; (*c*) M. Cornille and J. Horsley, *Chem. Phys. Lett.*, 1970, **6**, 373; (*d*) J. R. Sabin and H. Kim, *Chem. Phys. Lett.*, 1971, **11**, 593; (*e*) J. A. Pople, U. Seeger, R. Seeger and P. v. R. Schleyer, *J. Comput. Chem.*, 1980, **1**, 199; (*f*) J. S. Francisco and I. H. Williams, *Chem. Phys.*, 1985, **95**, 373.
9 P. LaBonville, R. Kugel and J. R. Ferraro, *J. Chem. Phys.*, 1977, **67**, 1477.
10 W. J. van de Guchte, J. P. Zwart and J. J. C. Mulder, *J. Mol. Struct.: THEOCHEM*, 1987, **152**, 213.

11 (*a*) M. A. Castro, S. Canuto and A. M. Simas, *Chem. Phys. Lett.*, 1991, **177**, 98; (*b*) R. D. J. Froese and J. D. Goddard, *J. Phys. Chem.*, 1993, **97**, 7484; (*c*) T. Kowalczyk and A. I. Krylov, *J. Phys. Chem. A*, 2007, **111**, 8271; (*d*) Y. Liu, I. B. Bersuker, W. Zou and J. E. Boggs, *J. Chem. Theory Comput.*, 2009, **5**, 2679; (*e*) C. Qin and T.-Y. Soo, *J. Mol. Struct.: THEOCHEM*, 2009, **897**, 32; (*f*) F. Grein, *J. Chem. Phys.*, 2013, **138**, 204305; (*g*) A. S. Averyanov, Y. G. Khait and Y. V. Puzanov, *J. Mol. Struct.: THEOCHEM*, 1999, **459**, 95.

12 A. M. Mebel, M. Hayashi, V. V. Kislov and S. H. Lin, *J. Phys. Chem. A*, 2004, **108**, 7983.

13 Review: R. I. Kaiser and A. M. Mebel, *Chem. Phys. Lett.*, 2008, **465**, 1.

14 C. J. Bennett, C. Jamieson, A. M. Mebel and R. I. Kaiser, *Phys. Chem. Chem. Phys.*, 2004, **6**, 735.

15 (*a*) P. G. Wenthold, J. Hu, R. R. Squires and W. C. Lineberger, *J. Am. Chem. Soc.*, 1996, **118**, 475; (*b*) P. G. Wenthold, J. Hu, R. R. Squires and W. C. Lineberger, *J. Am. Soc. Mass Spectrom.*, 1999, **10**, 800.

16 (*a*) T. Ichino, S. M. Villano, A. J. Gianola, D. J. Goebbert, L. Velarde, A. Sanov, S. J. Blanksby, X. Zhou, D. A. Hrovat, W. T. Borden and W. C. Lineberger, *Angew. Chem., Int. Ed.*, 2009, **48**, 8509; (*b*) T. Ichino, S. M. Villano, A. J. Gianola, D. J. Goebbert, L. Velarde, A. Sanov, S. J. Blanksby, X. Zhou, D. A. Hrovat, W. T. Borden and W. C. Lineberger, *J. Phys. Chem. A*, 2011, **115**, 1634.

17 P. G. Wenthold, J. B. Kim and W. C. Lineberger, *J. Am. Chem. Soc.*, 1997, **119**, 1354.

18 (*a*) Q. Fu, J. Yang and X.-B. Wang, *J. Phys. Chem. A*, 2011, **115**, 3201; (*b*) B. Chen, D. A. Hrovat, S. H. M. Deng, J. Zhang, X.-B. Wang and W. T. Borden, *J. Am. Chem. Soc.*, 2014, **136**, 3589; (*c*) R. C. Fort Jr, S. J. Getty, D. A. Hrovat, P. M. Lahti and W. T. Borden, *J. Am. Chem. Soc.*, 1992, **114**, 7549.

19 D. A. Hrovat, G.-L. Hou, X.-B. Wang and W. T. Borden, *J. Am. Chem. Soc.*, 2015, **137**, 9094.

20 C. D. Cappa and M. J. Elrod, *Phys. Chem. Chem. Phys.*, 2001, **3**, 2986.

21 R. G. Ewing and M. Waltman, *Int. J. Mass Spectrom.*, 2010, **296**, 53.

22 (*a*) D. E. Hunton, M. Hofmann, T. G. Lindeman and A. W. Castleman Jr, *J. Chem. Phys.*, 1985, **82**, 134; (*b*) J. T. Snodgrass, C. M. Roehl, A. M. van Koppen, W. E. Palke and M. T. Bowers, *J. Chem. Phys.*, 1990, **92**, 5935; (*c*) J. F. Hiller and M. L. Vestal, *J. Chem. Phys.*, 1980, **72**, 4713; (*d*) S. E. Novich, P. Engelking, P. L. Jones, J. H. Futrell and W. C. Lineberger, *J. Chem. Phys.*, 1979, **70**, 2652; (*e*) I. Dotan, J. A. Davidson, G. E. Streit, D. L. Albritton and F. C. Fehsenfeld, *J. Chem. Phys.*, 1977, **67**, 2874; (*f*) S. P. Hong, S. B. Woo and E. M. Helmy, *Phys. Rev. A*, 1977, **15**, 1563; (*g*) M. L. Vestal and G. H. Mauclaire, *J. Chem. Phys.*, 1977, **67**, 3758; (*h*) T. O. Tiernan and R. L. C. Wu, *Adv. Mass Spectrom.*, 1978, **7**, 136.

23 X.-B. Wang and L.-S. Wang, *Rev. Sci. Instrum.*, 2008, **79**, 073108.

24 Assuming the last phase to generate $CO_3^{\bullet-}$ from the Na_2CO_3 aqueous solutions in the electrospray ionization process is nanodroplets of waters containing one CO_3^{2-} solute, then we can estimate the ratio of CO_3^{2-} over HCO_3^- is about 0.1% from the known carbonic acid dissociation constants. Because $CO_3^{\bullet-}$ is derived from autodetachment of CO_3^{2-}, a weak intensity of $CO_3^{\bullet-}$ ion beam is expected.

25 B3LYP is a combination of Becke's 3-parameter hybrid exchange functional (A. D. Becke, *J. Chem. Phys*, 1993, **98**, 5648) with the electron correlation functional of Lee, Yang, and Parr (C. Lee, W. Yang and R. G. Parr, *Phys. Rev. B*, 1988, **37**, 785).

26 (*a*) G. D. Purvis and R. J. Bartlett, *J. Chem. Phys.*, 1982, **76**, 1910; (*b*) K. Raghavachari, G. W. Trucks, J. A. Pople and M. H. Head-Gordon, *Chem. Phys. Lett.*, 1989, **157**, 479.

27 K. Andersson, P.-Å. Malmqvist and B. O. Roos, *J. Chem. Phys.*, 1992, **96**, 1218.

28 W. T. Borden and E. R. Davidson, *Acc. Chem. Res.*, 1996, **29**, 87.

29 (*a*) T. H. Dunning Jr, *J. Chem. Phys.*, 1989, **90**, 1007; (*b*) R. A. Kendall, T. H. Dunning Jr and R. J. Harrison, *J. Chem. Phys.*, 1992, **96**, 6769.

30 M. J. Frisch, G. W. Trucks, H. B. Schlegel, G. E. Scuseria, M. A. Robb, J. R. Cheeseman, G. Scalmani, V. Barone, B. Mennucci, G. A. Petersson, H. Nakatsuji, M. Caricato, X. Li, H. P. Hratchian, A. F. Izmaylov, J. Bloino, G. Zheng, J. L. Sonnenberg, M. Hada, M. Ehara, K. Toyota, R. Fukuda, J. Hasegawa, M. Ishida, T. Nakajima, Y. Honda, O. Kitao, H. Nakai, T. Vreven, J. A. Montgomery Jr, J. E. Peralta, F. Ogliaro, M. Bearpark, J. J. Heyd, E. Brothers, K. N. Kudin, V. N. Staroverov, T. Keith, R. Kobayashi, J. Normand, K. Raghavachari, A. Rendell, J. C. Burant, S. S. Iyengar, J. Tomasi, M. Cossi, N. Rega, N. J. Millam, M. Klene, J. E. Knox, J. B. Cross, V. Bakken, C. Adamo, J. Jaramillo, R. Gomperts, R. E. Stratmann, O. Yazyev, A. J. Austin, R. Cammi, C. Pomelli, J. W. Ochterski, R. L. Martin, K. Morokuma, V. G. Zakrzewski, G. A. Voth, P. Salvador, J. J. Dannenberg, S. Dapprich, A. D. Daniels, O. Farkas, J. B. Foresman, J. V. Ortiz, J. Cioslowski and D. J. Fox, *Gaussian 09, Revision D.01*, Gaussian, Inc., Wallingford CT, 2013.

31 K. Andersson, F. Aquilante, M. Barysz, A. Bernhardsson, M. R. A. Blomberg, Y. Carissan, D. L. Cooper, M. Cossi, L. DeVico, N. Ferré, M. P. Fülscher, A. Gaenko, L. Gagliardi, G. Ghigo, C. de Graaf, S. Gusarov, B. A. Hess, D. Hagberg, A. Holt, G. Karlström, R. Lindh, P.-Å. Malmqvist, T. Nakajima, P. Neogrády, J. Olsen, T. Pedersen, M. Pitonak, J. Raab, M. Reiher, B. O. Roos, U. Ryde, B. Schimmelpfennig, M. Schütz, L. Seijo, L. Serrano-Andrés, P. E. M. Siegbahn, J. Stålring, T. Thorsteinsson, V. Veryazov and P.-O. Widmark, *MOLCAS version 7*, Lund University, Sweden, 2008.

32 V. A. Mozhayskiy and A. I. Krylov, *ezSpectrum, version 3.0*, see http://iopenshell.usc.edu/downloads.

33 (*a*) J. Franck, *Trans. Faraday Soc.*, 1926, **21**, 536; (*b*) E. Condon, *Phys. Rev.*, 1926, **28**, 1182.

34 Reviews: (*a*) L. C. Lineberger and W. T. Borden, *Phys. Chem. Chem. Phys.*, 2011, **13**, 11792; (*b*) W. T. Borden, in *Fifty Years of the James Flack Norris Award*, ed. E. T. Strom and V. Mainz, American Chemical Society, Washington, DC, in press.

35 (*a*) W. T. Borden and E. R. Davidson, *J. Am. Chem. Soc.*, 1977, **99**, 4587; (*b*) W. T. Borden, in *Diradicals*, ed. W. T. Borden, Wiley-Interscience, New York, 1982, pp. 1–72.

36 Review: W. Kutzelnigg, *Angew. Chem., Int. Ed. Engl.*, 1996, **35**, 573 and references therein.

37 Because the a_2'' π lone-pair MO contains bonding interactions between the 2p–π lone-pairs on the oxygens and the 2p–π AO on the carbon, it is considerably lower in energy than the σ and π lone-pair MOs on oxygen that are shown in Fig. 2.

38 As found previously,[20] a C_{2v} structure for $CO_3^{\bullet -}$ is computed to be higher in energy than the D_{3h} structure.

39 Review: E. R. Davidson and W. T. Borden, *J. Phys. Chem.*, 1983, **87**, 4783.

40 For more recent discussions of artifactual symmetry breaking in D_{3h} molecules, see (*a*) W. Eisfeld and K. Morokuma, *J. Chem. Phys.*, 2000, **113**, 5587; (*b*) C. E. Miller and J. W. Francisco, *J. Phys. Chem. A*, 2001, **105**, 1662; (*c*) Ref. 21.

41 Artifactual symmetry breaking leads to another phenomenon that can be seen in the results given in Table 1 for the triplet states. At D_{3h} geometries the E_x' and E_y' components of the $^3E'$ state should have identical energies, as should the E_x'' and E_y'' components of the $^3E''$ state. The fact that the two components of each degenerate state do not have exactly the same energies in Table 1 can be viewed as a consequence of the fact that, in general, electronic structure codes impose only C_{2v} symmetry on the MOs used to construct D_{3h} wave functions. Consequently, a wave function that nominally has E_x symmetry actually contains an A_2 contaminant; and a wave function that nominally has E_y symmetry actually contains an A_1 contaminant. Although the E_x and E_y components of such wavefunctions do have the same energies, the A_2 and A_1 contaminants do not; and this leads to the energy differences at D_{3h} geometries between the "E_x" and "E_y" states in Table 1.[39a]

42 See, *inter alia*, (*a*) U. Öpik and M. H. L. Pryce, *Proc. R. Soc. London, Ser. A*, 1957, **238**, 425; (*b*) R. F. W. Bader, *Can. J. Chem.*, 1962, **40**, 1164; (*c*) R. G. Pearson, *J. Am. Chem. Soc.*, 1969, **91**, 4947; (*d*) R. G. Pearson, *J. Mol. Struct.*, 1983, **103**, 25. For a recent review see: (*e*) I. B. Bersuker, *Chem. Rev.*, 2013, **113**, 1351.

43 H. A. Jahn and E. Teller, *Proc. R. Soc. London, Ser. A*, 1937, **161**, 220.

44 A similar situation occurs in the lowest energy triplet state of $(CO)_5$, which undergoes a first-order Jahn–Teller distortion from the D_{5h} geometry of the radical anion. The expected C–C bond stretching progression is, in fact, seen in the NIPE spectrum of $(CO)_5^{\bullet -}$ in the band for formation of the lowest triplet state of $(CO)_5$. X. Bao, D. A. Hrovat, W. T. Borden and X.-B. Wang, *J. Am. Chem. Soc.*, 2013, **135**, 4291.

45 C. J. Bennett, C. S. Jamieson and R. I. Kaiser, *Phys. Chem. Chem. Phys.*, 2010, **12**, 4032.